Photocatalysis in TiO$_2$ aqueous suspension: Effects of mono- or di-hydroxyl substitution of butanedioic acid on the disappearance and mineralisation rates

Wenny Irawaty[a], Donia Friedmann[a], Jason Scott[a], Pierre Pichat[b], Rose Amal[a,*]

[a] ARC Centre of Excellence for Functional Nanomaterials, School of Chemical Engineering, The University of New South Wales, Sydney, NSW 2052, Australia
[b] Photocatalyse et Environnement, CNRS/Ecole Centrale de Lyon (STMS), 69134 Ecully CEDEX, France

ARTICLE INFO

ABSTRACT

The photocatalytic degradation of butanedioic acid (BDA), hydroxybutanedioic acid (OH-BDA) and 2,3-dihydroxybutanedioic acid (diOH-BDA) (succinic acid, malic acid and tartaric acid, respectively) in a TiO$_2$ aqueous suspension at pH 3 was investigated to determine the effects of hydroxyl substitution. Temporal variations in the concentrations of the main intermediate products are reported. The use of a set of reactions involving decarboxylation and formation of alkylperoxy and alkoxy radicals has allowed us to account for the occurrence of these products, and to suggest the preferential decarboxylation of the COOH/COO$^-$ group adjacent to the OH group in OH-BDA. The adsorbed amounts in the dark increased with the number of OH groups, while the irradiation time necessary for total disappearance of the initial diacid, decreased. However, the evolution rate of CO$_2$, which was initially the same for the three acids, was then lower for the hydroxylated diacids for a significant period of irradiation time. This difference is tentatively attributed predominantly to the effect of hydroxyl substitution on the adsorption mode. One of the carboxyl groups would remain away from the surface (and hence not be available for direct electron transfer) due to the restricted mobility of the adsorbed diacid caused by hydrogen-bonding of TiO$_2$ with the alcohol group adjacent to the other carboxyl group. This hypothesis is also effective to qualitatively interpret how the zeta potential varied in the course of the degradation of each diacid. The present study further illustrates the essential role of distinct adsorption modes in photocatalytic events.

© 2011 Elsevier B.V. All rights reserved.

1. Introduction

Numerous articles and patents about TiO$_2$ photocatalysis have been published. Many reviews (for example [1–8] for 2009 and 2010 only) have also been issued concerning both the fundamentals and particular aspects of this field. The high bearing the target organic can have on governing photocatalyst performance, means recognising and understanding the factors influencing this aspect are important. For example, studies by Tran et al. [9] and Denny et al. [10] showed that even within an organic class, minor changes to the basic molecule structure can strongly influence photocatalyst performance. That is, changes to the molecule in terms of carbon chain length, chain branching and the varied presence of functional groups, as well as the nature, number and positions of substituents on benzene and other arene rings, could, in some cases, provide substantial differences in removal and mineralisation rates. In the present study, the mineralisation rate is defined as the CO$_2$ evolution rate measured during the photocatalytic reaction of the diacid.

Aliphatic acids are important raw materials for the manufacture of textiles, soaps, metallic materials and alcoholic or non-alcoholic beverages [11,12]. Carboxylic acids are often-encountered intermediate products of the oxidation of organic molecules en route to mineralisation of large molecules such as those contained in for example natural organic matter, pharmaceuticals, pesticides and dyes, and they are resistant to ordinary chemical oxidation. In addition, the ability of carboxylic acids to form complexes with toxic heavy metal ions is also of concern since this has been observed to increase the bioavailability of the heavy metal ions in the environment [13]. Furthermore, the presence of those acids at high concentration during chlorination in drinking water treatment could lead to generation of disinfection byproducts (DBPs) such as haloacetic acids that have been reported to be carcinogenic [14–16]. Therefore, the presence of any dissolved organic carbons (DOCs) including carboxylic acid molecules needs to be controlled before discharging to receiving waters.

This study is designed to elucidate the role that functional groups within a chosen aliphatic acid play in governing the removal and mineralisation rates using TiO$_2$ photocatalysis. The model molecules selected for the mechanistic investigation reported here are butanedioic acid and its mono-hydroxylated and symmetrical di-hydroxylated derivatives. These are commonly found in winery

wastewaters with typical pH between 3.65 and 5.40 [11,17]. It was thought that the presence, in addition to the carboxyl groups, of hydroxyl group(s) capable of forming hydrogen-bonds with TiO_2, should change the adsorption mode and, consequently, allows one to determine its role. To help validate our interpretation of the photocatalytic events, measurements of zeta potential were carried out before the irradiation was started and in the course of the photocatalytic degradation as these measurements provide information on the adsorption of charged molecules as previously demonstrated [18]. The reaction systems used in this study are, as usual in laboratory experiments, much simpler than those found in real wastewaters; however, the results from such experiments should help to identify important factors affecting the degradation of organic compounds in photocatalytic systems.

2. Experimental

2.1. Catalyst and chemicals

Aeroxide® TiO_2 P25 (primary particle size ~25 to 30 nm, surface area ~50 $m^2 g^{-1}$, anatase to rutile ratio of 4:1) was used as the photocatalyst since this TiO_2 specimen is most often used in photocatalytic studies. Chemicals were analytical or HPLC grade and used as supplied: butanedioic acid (>99%, Sigma–Aldrich®), hydroxybutanedioic acid (≥99%, Sigma–Aldrich®), 2,3-dihydroxybutanedioic acid (>99%, Sigma–Aldrich®), propanedioic acid (99%, Sigma–Aldrich®), ethanoic acid (99%, Ajax), hydroxyethanoic acid (99%, Sigma–Aldrich®), sodium dihydrogen phosphate (98%, M&B) and ammonium dihydrogen phosphate (98%, Ajax). Perchloric acid (70%, w/w in water, Frederick Chemical) and phosphoric acid (85%, w/w in water, Fluka) were used to control the pH of TiO_2 suspension and HPLC mobile phase, respectively. All solutions were prepared using ultra pure water (Millipore Milli-Q water).

2.2. Photocatalytic oxidation

Photocatalytic oxidation of BDA, OH-BDA and diOH-BDA were assessed in a 250 mL slurry spiral reactor as described previously [19]. Briefly, a 0.2 $g L^{-1}$ TiO_2 suspension (200 mL) was irradiated for 30 min to remove organic impurities from the TiO_2 surface. Then, the system was air-equilibrated prior to injecting 100 μL of the parent solution, corresponding to 2000 μg carbon (equivalent to 42 μmol of the parent acid). The solution was circulated for 20 min to allow for dark adsorption of the parent acid on the surface of TiO_2 before the light (Sylvania 18 W blacklight blue lamp with maximum emission of 365 nm) was switched on. The photocatalytic mineralisation reaction of the three diacids was monitored by recording the amount of carbon dioxide (CO_2) generated by means of an online conductivity meter (Jenway 4330). The experiments were repeated three times to ensure the reproducibility of the results. A TOC (total organic carbon) analyser was used to confirm complete mineralisation by measuring the concentration of total organic remaining in solution. HPLC (high performance liquid chromatography) was also used to analyse and identify the organic compounds left in the solution as the reaction progressed, while a zeta potential analyser was used to study the organics on the photocatalyst surface (details of the methods are given in Section 2.4).

2.3. Dark adsorption study

Dark adsorption experiments were performed in a 250 glass bottle at room temperature. BDA, OH-BDA and diOH-BDA solutions comprising 42 μmol (of each organic) were added to 200 mL of a 0.2 $g L^{-1}$ TiO_2 suspension (pH adjusted to 3 ± 0.05) and agitated by magnetic stirring for 20 min to promote adsorption/desorption

equilibrium at which time samples were collected for HPLC and zeta potential analyses.

2.4. Analytical methods

HPLC (Waters 2695) with a Photodiode Array Detector (Waters 2996) was used to identify organic compounds in solution. Samples were taken from the reactor and subsequently filtered through a 0.20 μm Millipore PTFE filter into small glass vials, capped and analysed by HPLC. An Atlantis T3 column (5 μm, 4.6 mm × 250 mm) was adopted to separate the compounds at 30 °C. The mobile phase was an aqueous solution of ammonium dihydrogen phosphate (pH 2.5) for identification of BDA, diOH-BDA and their intermediates, while sodium dihydrogen phosphate (pH 2.7) was used for OH-BDA and its intermediates. The separation of organics was performed under an isocratic condition with a mobile phase flow rate of 0.5 $mL min^{-1}$ and injection volume of 50 μL. Unknown organics were identified by comparing the retention times and UV spectra with pure standards. Linear calibration curves were obtained for organic concentrations in the range 0–12 ppm. TOC analysis was performed on a Shimadzu TOC-V_{CSH} analyser. Prior to analysis, the samples were filtered through the PTFE filter. Zeta potential analysis was used to monitor the presence of organics on the TiO_2 surface as the mineralisation reaction proceeded. Samples taken at selected time intervals were measured immediately using a Brookhaven Zeta-PALS analyser. The measurements were repeated in the absence of the parent acids to observe the effect of UV irradiation on the zeta potential of the photocatalyst.

3. Results and discussion

3.1. Results

3.1.1. Photocatalytic oxidation of the diacids

Control experiments (not shown) demonstrated no mineralisation of the diacids in the presence of TiO_2 without UV irradiation. Photolysis of the diacids was also not observed. Fig. 1(a, c and e) show CO_2 detected during the TiO_2 photocatalytic oxidation of BDA, OH-BDA and diOH-BDA, respectively, as a function of irradiation time (t_{UV}). Complete mineralisation of BDA, OH-BDA and diOH-BDA was achieved in approximately 30, 38 and 36 min, respectively. Additionally, TOC analysis employed at the end of the photocatalytic oxidation (results not shown) confirmed that the amount of organics remaining in solution was negligible. Also apparent in Fig. 1(a, c and e) is the three diacids have different photocatalytic mineralisation profiles. The BDA mineralisation profile follows a typical organic degradation profile, whereby the mineralisation rate gradually decreases with time, while OH-BDA and diOH-BDA have distinctive regions where the rates were constant for a period of time. Comparing the changing CO_2 generation rates (Fig. 1(a, c and e)) with intermediate product generation profiles (Fig. 1(b, d and f)) for each diacid demonstrates a relationship exists between the two, as expected. What is apparent is that the rate changes align with the appearance and disappearance of each particular intermediate product generated during degradation. Consequently, the regions depicted in Fig. 1(a–f) were selected based on the change in CO_2 generation rate. Three intermediate products (A_1, C_1 and C_2) in Fig. 1(b, d and f) could not be confirmed by comparison with commercial standards; therefore, they are presented as HPLC peak areas.

Complete mineralisation corresponded to the absence of any detected intermediate product for BDA and OH-BDA. This was not the case for diOH-BDA, for which no intermediate products were detected, under our analytical conditions, between 26 and 43 min irradiation time while CO_2 was still being generated. Complete
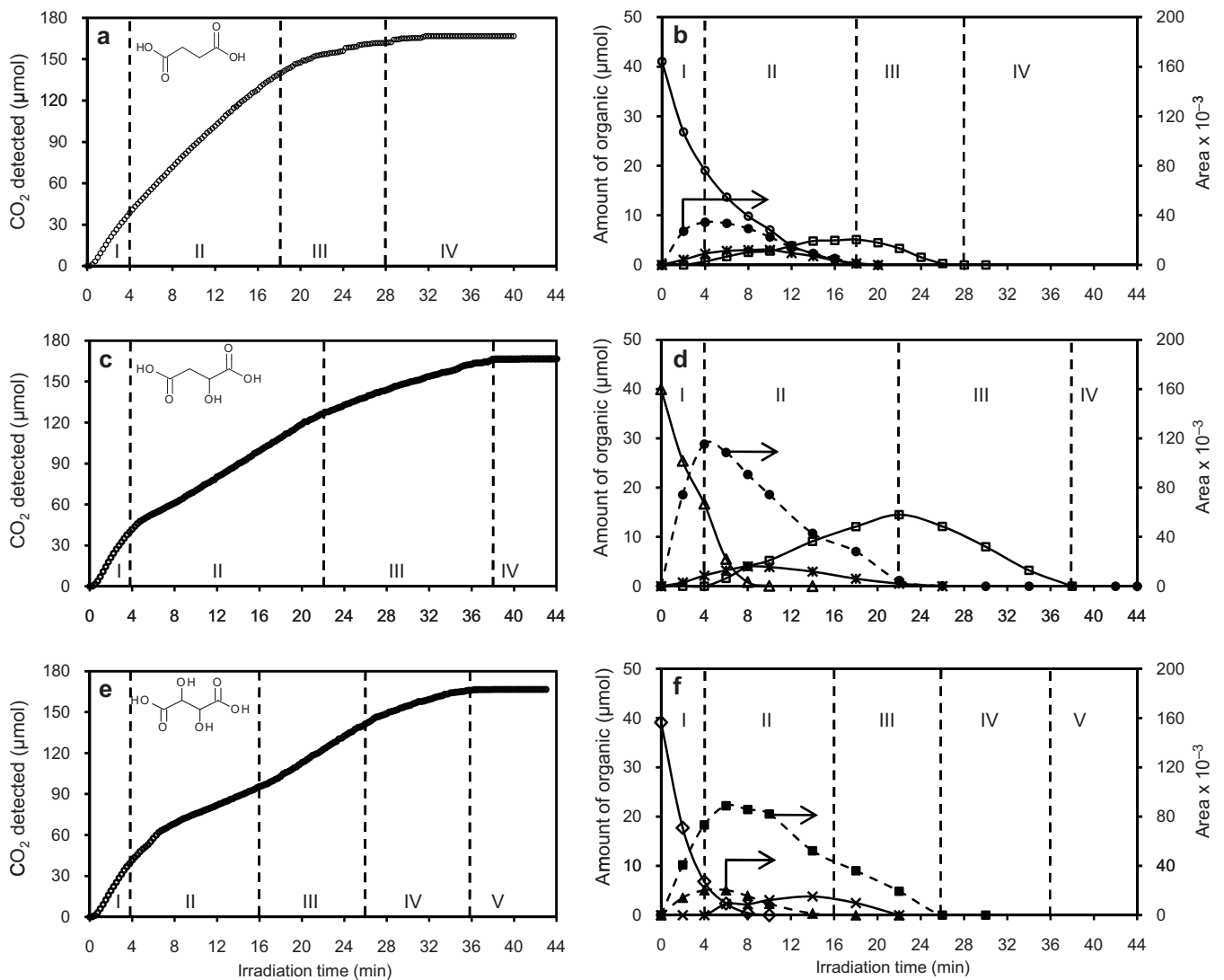
Fig. 1. (a, c, e) CO_2 generation profiles during photomineralisation of BDA, OH-BDA and diOH-BDA, respectively; (b, d, f) evolution and removal of intermediate compounds during irradiation of BDA, OH-BDA and diOH-BDA, respectively. (○) BDA; (△) OH-BDA; (◇) diOH-BDA; (✹) propanedioic acid; (□) ethanoic acid; (×) hydroxyethanoic acid; (●) intermediate A_1, believed to be 3-oxopropanoic acid [19]; (■) intermediate C_1; (▲) intermediate C_2. Unidentified intermediate profiles (dashed lines) are based on peak areas from HPLC chromatograms. Experimental conditions: TiO_2: $0.2\,g\,L^{-1}$; diacid initial amount: $42\,\mu mol$; initial pH: 3 ± 0.05.

disappearance of the diacid in solution corresponded to a change in the slope of the curve of the CO_2 amount against time for BDA only, possibly because this disappearance occurred when the remaining amounts of intermediate products were either nil or low (ethanoic acid).

3.1.2. Dark adsorption study

The adsorption on TiO_2 of BDA, OH-BDA and diOH-BDA in the dark was studied. The results (Fig. 2) indicate that the adsorbed amount is enhanced by additional OH functional group numbers on the carbon chain, as expected. Also shown in Fig. 2 is the TiO_2 zeta potential before and after dark adsorption of the diacids; it clearly shows that diOH-BDA imparted the greatest reduction to the TiO_2 surface charge, followed by OH-BDA, and that the variation due to BDA was low. This is proposed to reflect the greater adsorption of the carboxylate anions.

In this study, the initial suspension pH was set at 3 ± 0.05. At this pH, the TiO_2 surface is positively charged. The pH variation after the diacid adsorption was negligible. The amount of dissociated diacids in solution at pH 3, based on the pK_a values [20], is presented in Table 1. Approximately 50% of diOH-BDA exists in the
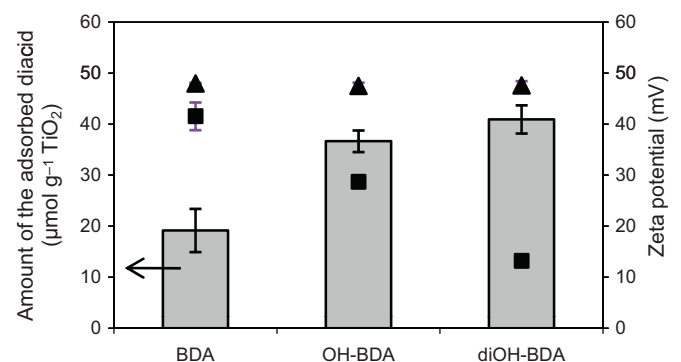

Fig. 2. The amounts of the diacid adsorbed on TiO_2 particles and the changes in TiO_2 zeta potential after organic adsorption. (▨) The amount of the adsorbed diacid on the surface of TiO_2; (▲) the initial TiO_2 zeta potential before adsorption; (■) the TiO_2 zeta potential after organic adsorption. Experimental conditions: TiO_2: $0.2\,g\,L^{-1}$; diacid initial amount: $42\,\mu mol$; initial pH: 3 ± 0.05; adsorption period: 20 min. Note that the TiO_2 has not undergone carbon burn off. While this is expected to affect the amount of adsorbed organics, and hence the measured zeta potential, the general trend shown here is expected to be upheld when comparing between the different organics.

Table 1
Dissociated structures and corresponding amounts for BDA, OH-BDA and diOH-BDA in water at 25 °C and pH 3.

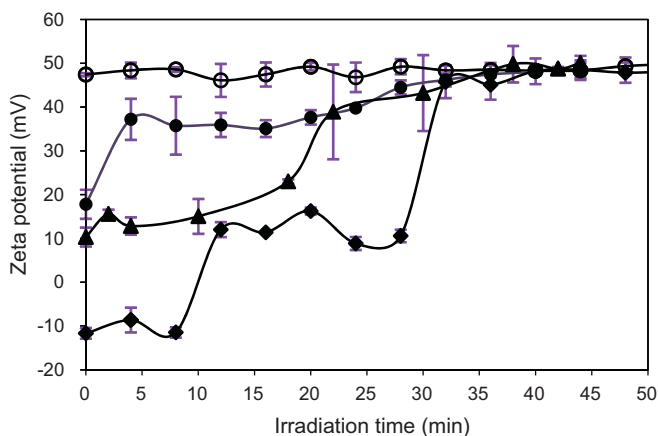| Substance	Dissociated species structures	Amount (%)
BDA	$HOOC–CH_2–CH_2–COO^-$	5.85
	$^-OOC–CH_2–CH_2–COO^-$	0.01
OH-BDA	$HOOC–CH_2–CHOH–COO^-$	25.83
	$^-OOC–CH_2–CHOH–COO^-$	0.21
diOH-BDA	$HOOC–CHOH–CHOH–COO^-$	47.93
	$^-OOC–CHOH–CHOH–COO^-$	2.02

Fig. 3. Change in TiO_2 zeta potential during irradiation of (○) aqueous TiO_2 suspension and TiO_2 suspension in the presence of: (●) BDA, (▲) OH-BDA and (♦) diOH-BDA. Experimental conditions: TiO_2: 0.2 g L^{-1}; diacid initial amount: 42 μmol; initial pH: 3 ± 0.05.

anionic form, favouring its adsorption through electrostatic attraction. For the other parent compounds, the amount of dissociated species in solution was 26 and 6% for OH-BDA and BDA, respectively. Thus, based on the pK_a values alone [20], it would be expected that diOH-BDA adsorbs to the greatest extent on TiO_2. In contrast to this finding, Chen et al. [21] reported no significant difference in the extent of adsorption of the same diacids at pH 2.9, on the same TiO_2, but at a much higher concentration so that the change in concentration due to adsorption might have been still more difficult to be measured.

The surface coverages at the initial concentration used in this study were 0.23, 0.41, and 0.50 molecules nm^{-2} for BDA, OH-BDA and diOH-BDA, respectively. With these low surface coverages, the degradation kinetics fitted the Langmuir–Hinshelwood model.

3.1.3. TiO_2 zeta potential during the reaction

TiO_2 zeta potential was measured during the diacid photocatalytic degradation (Fig. 3). This technique has been previously used to monitor the presence of adsorbed organics on the photocatalyst surface in bulk phase under irradiation [18]. The zeta potential of neat TiO_2 remained constant at value of ~+50 mV under irradiation. A comparison of the initial zeta potential values obtained for the different diacids shows that the additional OH functional groups led to a more negative zeta potential, which is indicative of greater adsorption of anions on the surface of TiO_2. The discrepancy between initial zeta potential values (time = 0) in Figs. 3 and 2 is believed to be due to the carbon burn off step (i.e., removal of adsorbed organic impurities) in the case of Fig. 3, which allowed a greater initial adsorption of the parent ionised diacids leading to a more negative initial TiO_2 zeta potential.

Within the first 4 min of irradiation, the TiO_2 zeta potential in the BDA system increases substantially from approximately +20 to +40 mV. This increase corresponds to the point where intermediate A_1 reached its maximum concentration (Fig. 1(b)). Beyond this

time there was a gradual return of the zeta potential to that of neat TiO_2. The profile suggests either low levels of mildly adsorbed organics (e.g. intermediate A_1) and/or weakly adsorbed organics (e.g. ethanoic acid) are present on the TiO_2 surface during BDA photodegradation.

A detailed description of OH-BDA photodegradation in relation to zeta potential is described in a previous publication [19]. Briefly, there is little change in the zeta potential upon irradiation until around the 22 min mark where a significant increase is observed. This represents the time at which intermediate A_1 and propanedioic acid are removed from the system and ethanoic acid is dominant (Fig. 1(d)). Despite similar intermediates being detected as in the BDA system, extended lower value of the zeta potential for OH-BDA may be due to the higher concentrations observed for these intermediates during irradiation.

On irradiation of the diOH-BDA system, the zeta potential remained at ~−10 mV for 8 min after which it increased to ~+10 mV. According to Fig. 1(f), this time corresponded to complete diOH-BDA removal and the peak maximum for intermediate C_1. The zeta potential remained steady ~+10 mV until t_{UV} = 28 min, with this time corresponding approximately to the time at which all intermediates were consumed. Beyond this time the zeta potential returned to the neat TiO_2 value indicating most traces of organics had been removed from the surface.

3.2. Discussion

3.2.1. Degradation pathways

To highlight the similarities and differences in the degradation pathways of the studied diacids, we first indicate the typical reactions that are expected, and then apply these reactions to each butanedioic acid.
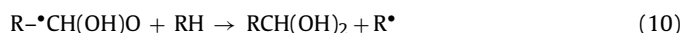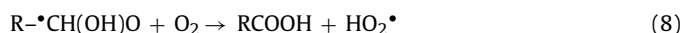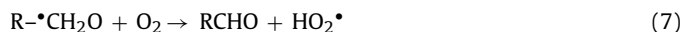
The degradation of carboxylate anions and carboxylic acids is believed to occur through the photo-Kolbe reaction [22]:

$$RCOO^- + h^+ \rightarrow R^\bullet + CO_2 \tag{1}$$

$$RCOOH + h^+ \rightarrow R^\bullet + H^+ + CO_2 \tag{2}$$

The reaction pathways of an organic radical $R^\bullet$ are well documented [23–25]. They include addition of O_2, abstraction of H atoms and cleavages. In the presence of O_2, alkyl radicals are transformed into alkylperoxy (Eq. (3)) and alkoxy radicals (Eq. (4)), as is shown by the main overall equations:

$$R^\bullet + O_2 \rightarrow RO_2^\bullet \tag{3}$$

$$2RO_2^\bullet \rightarrow 2RO^\bullet + O_2 \text{ and } RO_2^\bullet + RH \rightarrow ROOH + R^\bullet;$$

$$ROOH \rightarrow RO^\bullet + {}^\bullet OH \tag{4}$$

Depending on the chemical structure of the $RO^\bullet$, namely in the present case either $R–{}^\bullet CH_2O$ or $R–{}^\bullet CH(OH)O$, the following reactions are suggested to take place:

$$R–{}^\bullet CH_2O \rightarrow RCHO + H^\bullet \tag{5}$$

$$R–{}^\bullet CH(OH)O \rightarrow RCOOH + H^\bullet \tag{6}$$

$$R–{}^\bullet CH_2O + O_2 \rightarrow RCHO + HO_2^\bullet \tag{7}$$

$$R–{}^\bullet CH(OH)O + O_2 \rightarrow RCOOH + HO_2^\bullet \tag{8}$$

$$R–{}^\bullet CH_2O + RH \rightarrow RCH_2OH + R^\bullet \tag{9}$$

$$R–{}^\bullet CH(OH)O + RH \rightarrow RCH(OH)_2 + R^\bullet \tag{10}$$
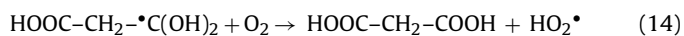
$$RCH(OH)_2 \rightleftharpoons RCHO + H_2O \tag{11}$$

It is important to underline that these reactions involve either no oxidant (Eqs. (4)–(6) and (9)–(11)) or only O_2 (Eqs. (3), (7), (8)),
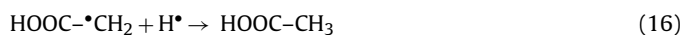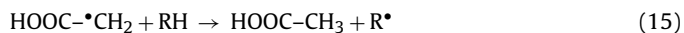
and no h$^+$ or $^\bullet$OHs. Accordingly, their probability of occurring is high. Moreover, regarding the RO$^\bullet$s, their decomposition (Eqs. (5) and (6)) and their reactions with O_2 (Eqs. (7) and (8)) are more probable than their reactions with organic molecules (Eqs. (9) and (10)) whose concentration is much lower than that of O_2.

In the following sections we successively indicate which products can be formed from each of the diacids studied according to the pathways corresponding to Eqs. (1)–(11).

3.2.1.1. Case of butanedioic acid (BDA). Given the symmetric structure of BDA (inset in Fig. 1(a)), decarboxylation can take place at either of the two COOH/COO$^-$ groups in the carbon chain. Consequently, CO_2 is evolved and a carbon-centred radical is formed (Eqs. (1) and (2)). The R$^\bullet$ being HOOC–CH$_2$–$^\bullet$CH$_2$, the expected product is HOOC–CH$_2$–CHO (3-oxopropanoic acid; Eqs. (3)–(5) and (7)), which was tentatively identified to correspond to intermediate A$_1$ (Fig. 1(b)), whereas the formation of HOOC–CH$_2$–CH$_2$OH (Eqs. (3), (4), (9)) is less probable and, in fact, this potential intermediate product was not observed, at least under our analytical conditions. Oxidation of 3-oxopropanoic acid can easily occur upon $^\bullet$OH attack of the gem-diol resulting from hydration of the aldehyde group (Eqs. (12)–(14)). This leads to propanedioic acid, which was observed in the solution (Fig. 1(b)):

$$HOOC–CH_2–CHO + H_2O \leftrightharpoons HOOC–CH_2–CH(OH)_2 \quad (12)$$

$$HOOC–CH_2–CH(OH)_2 + {}^\bullet OH \rightarrow HOOC–CH_2–{}^\bullet C(OH)_2 + H_2O \quad (13)$$

$$HOOC–CH_2–{}^\bullet C(OH)_2 + O_2 \rightarrow HOOC–CH_2–COOH + HO_2^\bullet \quad (14)$$

The formation of ethanoic acid (Fig. 1(b)) implies both the breaking of a C–C bond and the addition of a H atom to obtain the CH$_3$ group. The C–C bond breaking can result from the decarboxylation of propanedioic acid or its anions (Eqs. (1) and (2)) yielding HOOC–$^\bullet$CH$_2$, while the H atom can be abstracted from a BDA molecule (Eq. (15)) or stem from Eq. (5):

$$HOOC–{}^\bullet CH_2 + RH \rightarrow HOOC–CH_3 + R^\bullet \quad (15)$$

$$HOOC–{}^\bullet CH_2 + H^\bullet \rightarrow HOOC–CH_3 \quad (16)$$

3.2.1.2. Case of dihydroxybutanedioic acid (diOH-BDA). In the case of diOH-BDA, because of the symmetrical chemical structure of this diacid (inset in Fig. 1(e)), the R$^\bullet$ (Eqs. (1) and (2)) can only be HOOC–CHOH–$^\bullet$CHOH. From this radical, the expected products are HOOC–CHOH–COOH (hydroxypropanedioic acid; Eqs. (3), (4), (6), (8)) and HOOC–CHOH–CHO (2-hydroxy-3-oxopropanoic acid; Eqs. (3), (4), (10), (11)). None of the chromatographic peaks can be attributed to hydroxypropanedioic acid whose retention time (t_r) was 6.3 min under our analytical conditions. In the absence of a commercial standard, the t_r of HOOC–CHOH–CHO can only be deduced by analogy. Given that t_r of HOOC–CH$_2$–CHO was 7.7 min, it is tentatively suggested that the intermediate product C$_1$ (t_r = 7.6 min; Fig. 1(f)) might be HOOC–CHOH–CHO.

It could be envisaged that HOOC–CHOH–COOH was oxidised to a diol-diacid (HOOC–C(OH)$_2$–COOH (dihydroxypropanedioic acid)) by the removal, through a $^\bullet$OH attack, of the relatively labile H atom carried by the central C atom, followed by processes corresponding to Eqs. (3) and (4) leading to the radical HOOC–C(OH)$^\bullet$O–COOH and then:

$$HOOC–{}^\bullet C(OH)O–COOH + RH \rightarrow HOOC–C(OH)_2–COOH + R^\bullet \quad (17)$$
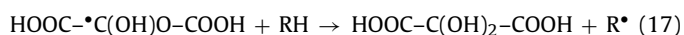
However, this product was not detected. Although the C$_2$ intermediate product possessed the same retention time (8 min) as HOOC–C(OH)$_2$–COOH, its UV spectrum differed. On the other hand, the relatively low concentration reached by this intermediate C$_2$ may indeed indicate that it was a secondary oxidation product and that its formation would compete with that of hydroxyethanoic acid as indicated in the following paragraph.

As in the case of the formation of ethanoic acid from BDA, the observed formation of hydroxyethanoic acid from diOH-BDA implies an additional C–C bond breaking via the decarboxylation of hydroxypropanedioic acid and reactions equivalent to those corresponding to Eqs. (15) and (16) for the resulting radical HOOC–$^\bullet$CHOH. Consequently, hydroxypropanedioic acid can lead to both dihydroxypropanedioic acid and hydroxyethanoic acid, which might explain why it was not detected. In addition, given the pK_{a1} and pK_{a2} values of hydroxypropanedioic acid of 2.37 and 4.74, respectively [20], approximately 82.5% of the acid is dissociated at pH 3 and will most likely be easily adsorbed on the positively charged surface of TiO$_2$, hence avoiding detection in solution.

3.2.1.3. Case of hydroxybutanedioic acid (OH-BDA). When OH-BDA was employed as the starting reactant, depending on whether the initial decarboxylation concerns the carboxylic group adjacent to either the CHOH group or the CH$_2$ group, the R$^\bullet$ (Eqs. (1) and (2)) is suggested to be either HOOC–CH$_2$–$^\bullet$CHOH or HOOC–CHOH–$^\bullet$CH$_2$.

The expected products of HOOC–CH$_2$–$^\bullet$CHOH are HOOC–CH$_2$–COOH (propanedioic acid; Eqs. (3), (4), (6), (8)) and HOOC–CH$_2$–CHO (3-oxopropanoic acid; Eqs. (3), (4), (10), (11)). As presented in Fig. 1(d), propanedioic acid was identified, while 3-oxopropanoic acid – reported to be the main intermediate product of OH-BDA [26] – was believed to be intermediate A$_1$ [19]. Alternatively, the former product can also result from the latter product through oxidation involving $^\bullet$OH (Eqs. (12)–(14)), which is less probable. The same reactions as in the case of BDA would lead to the formation of ethanoic acid.

In fact, although the R$^\bullet$ issued from Eqs. (1) and (2) was different (HOOC–CH$_2$–$^\bullet$CHOH in place of HOOC–CH$_2$–$^\bullet$CH$_2$), the identified products from OH-BDA and BDA were the same. However, according to the pathways proposed, propanedioic acid requires further oxidation by a $^\bullet$OH, to be formed from BDA via 3-oxopropanoic acid (Eqs. (12)–(14)), whereas it can also be formed from OH-BDA without involving $^\bullet$OH. However, that was not reflected by the temporal variations in the low concentration of propanedioic acid, which were similar in both cases (Fig. 1(b and d)).

By contrast, the radical HOOC–CHOH–$^\bullet$CH$_2$ – resulting from the decarboxylation of the COOH/COO$^-$ group adjacent to the CH$_2$ group – would lead first to HOOC–CHOH–CH$_2$O$^\bullet$ (Eqs. (3) and (4)) and then to HOOC–CHOH–CHO (2-hydroxy-3-oxopropanoic acid) by both Eq. (5) and (7) and to HOOC–CHOH–CH$_2$OH (2,3-dihydroxypropanoic acid) via a less probable reaction (Eq. (9)). Additionally, oxidation of HOOC–CHOH–CHO would have produced HOOC–CHOH–COOH (Eqs. (12)–(14)). None of these three products were detected.

These observations strongly suggest that decarboxylation predominantly occurs at the COOH/COO$^-$ group adjacent to the CHOH group thus leading to the radical HOOC–CH$_2$–$^\bullet$CHOH. This is not unexpected because the OH group of OH-BDA can easily form a hydrogen bond with the surface OH groups of TiO$_2$. Consequently, the adjacent COOH/COO$^-$ group would also be more easily bound to TiO$_2$ and hence more susceptible to react with h$^+$ (Eqs. (1) and (2)). By contrast, the other COOH/COO$^-$ group would be more distant from the surface and hence not prone to direct electron transfer. This type of reasoning is further developed in the following sections.

To conclude this section, the use of a set of reactions has allowed us to explain the formation of the three acids (3-oxopropanoic, propanedioic and ethanoic acids) that were identified in the course of the degradation of BDA and OH-BDA, and to propose that the initial decarboxylation of OH-BDA occurred preferentially at the position adjacent to the alcohol group. In the case of diOH-BDA, hydroxypropanedioic acid was not detected although its formation was forecasted according to the same set of reactions, possibly because it was rapidly transformed into dihydroxypropanedioic

acid and hydroxyethanoic acid and/or because of its high ionisation percentage it remained predominantly adsorbed. Also, the formation of 2-hydroxy-3-oxopropanoic acid suggested from the set of reactions was not certain in the absence of a standard.

3.2.2. Mineralisation rates

For the three diacids, the amount of CO_2 detected in the system was almost the same over approximately the first 4 min of irradiation (Fig. 1(a, c and e)). As decarboxylation is very likely the easiest mineralisation pathway (Eqs. (1) and (2)), it should contribute the most to CO_2 generated during this initial period. To wit, no intermediate products still containing the two initial $COOH/COO^-$ groups were detected.

The higher mineralisation rate of BDA, observed between $4 < t_{UV} < 16$ min, can be explained by several reasons. One of the reasons could be easier decarboxylation of the second $COOH/COO^-$ group for BDA than the hydroxylated diacids. To account for this easier decarboxylation of BDA, it is hypothesized that the formation of a hydrogen bond between TiO_2 and the OH group of OH-BDA maintains the COOH group not adjacent to the OH group away from the surface and thus hinders its decarboxylation. In the case of diOH-BDA, the two OH groups point in opposite directions, so that only one of these groups can easily be hydrogen-bound to TiO_2; accordingly, the situation is equivalent to that of OH-BDA, that is, one of the COOH group is not close to the surface. By contrast, the absence of a OH group in BDA allows both COOH groups to interact with TiO_2 indifferently. In other words, the suggested difference in the adsorption mode of BDA and the hydroxylated diacids might explain why the CO_2 generated was higher for BDA in region II despite a lower oxidation state of the non-carboxylic C atoms and a lower extent of adsorption (Fig. 2). This is a case where molecules that are less mobile at the solid surface reduce the possibilities of attack at several molecular positions by surface-located active species and, consequently, can decrease the mineralisation rate.

Additionally, up to $t_{UV} = 8$ min – which corresponded to the disappearance of either OH-BDA or diOH-BDA – the TiO_2 agglomerates were surrounded by ionised molecules of these diacids as shown by the zeta potential measurements discussed in the following section. This phenomenon might have facilitated desorption of the intermediate products – which all contained a $COOH/COO^-$ group – and, accordingly, delayed their decarboxylation. The higher concentration reached by 3-oxopropanoic acid issued from OH-BDA than from BDA (Fig. 1(d) and (b), respectively) and also the temporal variation of intermediate C_1 (unfortunately, not quantified) formed from diOH-BDA (Fig. 1(f)) may lend support to this interpretation.

3.2.3. Zeta potential variations

The initial zeta potential values ($t_{UV} = 0$) showed that the TiO_2 surface charge was more negative with a greater adsorption of the more hydroxylated diacid (Fig. 3). The solution concentration of OH^-, that is, 10^{-11} mol L^{-1} at pH 3, was negligible with respect to the initial diacid concentration (2.08×10^{-4} mol L^{-1}). Consequently, the TiO_2 surface charge depended on the mono- or di-ionised diacid concentration at pH 3 (Table 1) and indeed the zeta potential varied with this concentration, although not proportionally (see the next paragraph for a tentative interpretation).

The difference in surface charge with respect to an aqueous suspension of TiO_2 considerably decreased over about the first 5 min of irradiation when the starting reactant was BDA, whereas it remained the same when it was OH-BDA or diOH-BDA (Fig. 3). The origin of this contrasting behaviour could be, in the case of the hydroxylated diacids, a faster replacement at the TiO_2 surface of the ionised diacid that has been degraded by non-degraded ionised diacid. Indeed, two arguments can be put forward in favour of a faster replacement. First, on the basis of the percentages of ionised

molecules (Table 1), the fraction of diacid molecules attracted to TiO_2 by electrostatic forces was about 1/2 for diOH-BDA, 1/4 for OH-BDA and only 1/16 for BDA, which meant much higher probabilities of hitting the surface for the ionised hydroxylated diacids. Second, it seems reasonable to propose that the residence time of the ionised hydroxylated diacids at the surface would be increased by the possibility of forming an additional hydrogen bond with TiO_2 via the alcohol group as mentioned in the previous sections. For diOH-BDA, the increase in residence time should be even more pronounced than for OH-BDA because this possibility exists whatever the COO^- anion hitting the surface; this reasoning may explain why the initial zeta potential caused by these hydroxylated diacids differed more than expected from the respective ionised fractions (Table 1).

After the initial increase in zeta potential, no significant change occurred until about $t_{UV} = 22$ min when the starting reactant was BDA (Fig. 3). The corresponding zeta potential value was around +40 mV against +50 mV for an aqueous suspension of TiO_2. This small difference is supposed to be due to the adsorption of ionised remaining BDA (up to 18 min; Fig. 1(b)) and carboxylate anions of the intermediate products. The zeta potential reached +50 mV at $t_{UV} > 32$ min showing the total elimination of negatively charged intermediate products, which was consistent with the achievement of the maximum concentration in CO_2 as a function of t_{UV} (Fig. 1(a)) because the near-to-complete-mineralisation products are assumed to be carboxylic acids.

When the starting reactant was OH-BDA, a progressive increase in zeta potential was observed beyond 8 min, this time corresponding to the complete disappearance of OH-BDA in solution. However, the zeta potential attained the same value as in the case of BDA only after about 22 min. It is suggested that this difference may have been caused by a higher concentration in ionised intermediate products, especially 3-oxopropanoate and ethanoate anions (Fig. 1(d)). Also, note that the zeta potential reached +50 mV at the same time (about 38 min; Fig. 3) as the achievement of the maximum concentration in CO_2 (Fig. 1(c)).

In the case of diOH-BDA as the starting reactant, an increase in zeta potential from about −10 mV to +12 mV was observed once diOH-BDA was no longer detected in the solution, that is, beyond about $t_{UV} = 8$ min (Fig. 1(f)). The value reached was approximately the same as that found initially when OH-BDA was the starting molecule (Fig. 3). It may mean that the corresponding density in COO^- groups at the surface depended on the presence of an adjacent OH group in the intermediate products, which should be the case given the formula of diOH-BDA. Indeed, hydroxyethanoic acid was identified, dihydroxypropanedioic acid was presumed to be formed and 2-hydroxy-3-oxopropanoic acid was tentatively suggested to be generated. As aforementioned, this adjacent OH group would increase the residence time of carboxylate anions at the surface. The zeta potential value of about +10–12 mV ($t_{UV} = 12$–26 min; Fig. 3), attributed mainly to hydroxylated carboxylate anions, was maintained until the intermediate products had disappeared at $t_{UV} = 26$–28 min (Fig. 1(f)). The zeta potential value of an aqueous suspension of TiO_2 was then reached at a time approximately corresponding to total mineralisation (Fig. 1(e)), as was expected.

It is clear here that the zeta potential variations not only reflected the concentrations in the initial reactant and intermediate products – which were all carboxylic acids – but also the longer residence time of these compounds on the TiO_2 surface when an alcohol group was adjacent to the carboxylate group. The conclusions drawn from these measurements are consistent with both the selectivity – deduced from the pathways we have proposed – for the decarboxylation of OH-BDA and the adsorption modes suggested to interpret the distinct mineralisation rates of the three diacids studied.

4. Conclusions

In an effort to further illustrate the impact of adsorption modes in photocatalysis of aliphatic acids, this study focused on determining to what extent the substitution of one hydroxyl group or two hydroxyl groups at different positions in BDA – which should change the binding to the TiO_2 surface – affected the disappearance rates, possible competitive adsorption with the intermediate products and the mineralisation rates. To interpret the apparent discrepancies found between the adsorbed amounts in the dark and the photocatalytic disappearance rates on one side, and the mineralisation kinetics on the other side, it is hypothesised that the hydroxyl substitution modifies the type of adsorption, the associated geometry and the mobility in the adsorbed phase, so that the average distance between the surface and one of the carboxyl groups would increase. Accordingly, the possibility of surface-located direct electron transfer, believed to effect decarboxylation, would be hindered for this carboxyl group. This hypothesis is supported by zeta potential measurements. The initial zeta potential values and those recorded in the course of the photocatalytic degradation can indeed be explained by assuming that the residence time of a carboxylate anion near the surface is increased by the presence of a vicinal hydroxyl group. Although it does not provide direct information on the nature of the low adsorbed species and on the adsorption modes, electrophoresis proves, nevertheless, to be instructive about the ability of the charged molecules to bind to the surface. This investigation shows that, in practice, higher removal rates of target pollutants, even those having common structural moieties, do not warrant higher mineralisation rates of these pollutants.

Acknowledgements

References

[1] Y. Paz, Photocatalytic treatment of air: from basic aspects to reactors, in: H.I. de Lasa, B.S. Rosales (Eds.), Adv. Chem. Eng., Academic Press, Amsterdam, 2009, pp. 289–336.
[2] H. Zhang, G. Chen, D.W. Bahnemann, J. Mater. Chem. 19 (2009) 5089–5121.
[3] D. Friedmann, C. Mendive, D. Bahnemann, Appl. Catal. B 99 (2010) 398–406.
[4] Y. Paz, Appl. Catal. B 99 (2010) 448–460.
[5] P. Pichat, Appl. Catal. B 99 (2010) 428–434.
[6] Y. Paz, Solid State Phenomena 162 (2010) 135–162.
[7] D. Mitoraj, H. Kisch, Solid State Phenomena 162 (2010) 49–75.
[8] P. Pichat, J. Adv. Oxid. Technol. 13 (2010) 238–246.
[9] H. Tran, J. Scott, K. Chiang, R. Amal, J. Photochem. Photobiol. A 183 (2006) 41–52.
[10] F. Denny, J. Scott, K. Chiang, W.Y. Teoh, R. Amal, J. Mol. Catal. A 263 (2007) 93–102.
[11] T. Colin, A. Bories, Y. Sire, R. Perrin, Water Sci. Tehnol. 51 (2005) 99–106.
[12] N. Quichi, M.E. Morgada, G. Piperata, P. Babay, R.T. Gettar, M.I. Litter, Catal. Today 101 (2005) 253–260.
[13] A.P. Schwab, D.S. Zhu, M.K. Banks, Chemosphere 72 (2008) 986–994.
[14] K. Gopal, S.S. Tripathy, J.L. Bersillon, S.P. Dubey, J. Hazard. Mater. 140 (2007) 1–6.
[15] U.S. Environmental Protection Agency, Basic information about disinfection byproducts in drinking water: total trihalomethanes, haloacetic acids, bromate, and chlorite. http://water.epa.gov/drink/contaminants/basicinformation/disinfectionbyproducts.cfm (accessed 30.06.2011).
[16] C.M. Villanueva, M. Kogevinasa, J.O. Grimalt, Water Res. 37 (2003) 953–958.
[17] A. Versari, M. Castellari, U. Spinabelli, S. Galassi, J. Chem. Technol. Biotechnol. 76 (2001) 485–488.
[18] S.W. Lam, K. Chiang, T.M. Lim, R. Amal, G.K.-C. Low, J. Photochem. Photobiol. A 187 (2007) 127–132.
[19] W. Irawaty, D. Friedmann, J. Scott, R. Amal, J. Mol. Catal. A 335 (2011) 151–157.
[20] G.W. Gokel, Dean's Handbook of Organic Chemistry, second ed., McGraw-Hill, New York, 2004.
[21] Q. Chen, J.M. Song, F. Pan, F.L. Xia, J.Y. Yuan, Environ. Technol. 30 (2009) 1103–1109.
[22] B. Kraeutler, A.J. Bard, J. Am. Chem. Soc. 100 (1978) 5985–5992.
[23] C. von Sonntag, H.-P. Schuchmann, Angew. Chem. Int. Ed. 30 (1991) 1229–1253.
[24] K. Stemmler, U. von Gunten, Atm. Environ. 34 (2000) 4241–4252.
[25] C. von Sonntag, Free-radical-induced DNA Damage and its Repair: A Chemical Perspective, Springer, Berlin, 2006.
[26] J.-M. Herrmann, H. Tahiri, C. Guillard, P. Pichat, Catal. Today 54 (1999) 131–141.